arXiv:2301.10820v3 [cond-mat.mes-hall] 23 Jun 2023

Two-photon excitation with finite pulses unlocks pure dephasing-induced degradation of entangled photons emitted by quantum dots

T. Seidelmann,[1,*] T. K. Bracht,[2,3] B. U. Lehner,[4,5] C. Schimpf,[4] M. Cosacchi,[1] M. Cygorek,[6] A. Vagov,[1] A. Rastelli,[4] D. E. Reiter,[3] and V. M. Axt[1]

[1] *Lehrstuhl für Theoretische Physik III, Universität Bayreuth, 95440 Bayreuth, Germany*
[2] *Institut für Festkörpertheorie, Universität Münster, 48149 Münster, Germany*
[3] *Condensed Matter Theory, Department of Physics, TU Dortmund, 44221 Dortmund, Germany*
[4] *Institute of Semiconductor and Solid State Physics, Johannes Kepler University Linz, 4040 Linz, Austria*
[5] *Secure and Correct Systems Lab, Linz Institute of Technology, 4040 Linz, Austria*
[6] *Heriot-Watt University, Edinburgh EH14 4AS, United Kingdom*

Semiconductor quantum dots have emerged as an especially promising platform for the generation of polarization-entangled photon pairs. However, it was demonstrated recently that the two-photon excitation scheme employed in state-of-the-art experiments limits the achievable degree of entanglement by introducing which-path information. In this work, the combined impact of two-photon excitation and longitudinal acoustic phonons on photon pairs emitted by strongly-confining quantum dots is investigated. It is found that phonons further reduce the achievable degree of entanglement even in the limit of vanishing temperature due to phonon-induced pure dephasing and phonon-assisted one-photon processes, which increase the reexcitation probability. In addition, the degree of entanglement, as measured by the concurrence, decreases with rising temperature and/or pulse duration, even if the excitonic fine-structure splitting is absent and when higher electronic states are out of reach. Furthermore, in the case of finite fine-structure splittings, phonons enlarge the discrepancy in concurrence for different laser polarizations.

I. INTRODUCTION

In the past decades, many fascinating applications emerged in novel quantum technologies, such as quantum cryptography [1–4], quantum communication [5], or quantum information technology and computing [6–9], that are based on the concept of entanglement, a genuine quantum phenomenon. Especially entangled photons attracted a lot of interest as photons travel at the speed of light and are hardly influenced by their environment [10]. Semiconductor quantum dots (QDs) show the potential to be an excellent on-demand source of high-quality polarization-entangled photon pairs, as demonstrated in various experiments [11–29] and theoretical studies [30–37].

Focusing on its biexciton-exciton cascade, a QD represents a quantum emitter with four levels in a diamond configuration (cf. Fig. 1), that, in principle, is able to generate maximally entangled photon pairs. After the preparation of the biexciton state, two photons are emitted while the QD relaxes back into its ground state. Because there exist two different exciton states, this relaxation can take two different paths, resulting in the creation of either two horizontally (H) or two vertically (V) polarized photons. Thus, in an ideal situation, i.e., when both decay paths are otherwise indistinguishable, a maximally entangled two-photon state

$$|\Phi_+\rangle = \left(|HH\rangle + |VV\rangle\right)/\sqrt{2} \tag{1}$$

is generated. However, in typical QDs, the exchange interaction causes the two exciton states to be energetically split by the so-called fine-structure splitting (FSS). Due to the FSS, the emitted photons can be distinguished by their energies. Thus, the FSS introduces which-path information into the system as both decay paths are no longer indistinguishable, resulting in a reduced degree of entanglement. In the measured two-photon state, this which-path information manifests itself as a reduced coherence between the states $|HH\rangle$ and $|VV\rangle$ caused by a time-dependent phase oscillation between the exciton states with a frequency proportional to the magnitude of the FSS [38].

Several approaches to eliminate the FSS have been pursued [15, 17, 22, 23] and state-of-the-art experiments employing resonant two-photon excitation (TPE) have reported unprecedented degrees of entanglement [3, 21–26, 39]. However, a perfectly entangled two-photon state $|\Phi_+\rangle$ has not yet been observed. Rather, it was shown recently that the TPE scheme itself limits the achievable degree of entanglement by introducing an energy splitting between the exciton states via the AC Stark effect, and thus which-path information, during the duration of the excitation pulse [40, 41].

In contrast to other possible realizations of a four-level quantum emitter, like F-centers or atoms [42–44], QDs unavoidably interact with their semiconductor environment, giving rise to electron-phonon interactions. The pure dephasing-type coupling to longitudinal acoustic (LA) phonons in strongly-confining QDs was shown to impact the entanglement of emitted photon pairs in the case of finite which-path information. Depending on other system parameters, the phonon impact can range

* Corresponding author: tim.seidelmann@uni-bayreuth.de

from phonon-induced enhancement [35] over a partially reduced degree of entanglement [32] to a complete loss of entanglement, which takes place for strong constant excitation [45]. Note that for completely symmetric level structures without FSS, pure dephasing does not reduce the degree of entanglement when an initially prepared biexciton is assumed [30–32]. However, this may change when the finite time of the excitation process is explicitly taken into account, especially because the TPE scheme itself introduces which-path information. In particular, it has previously been demonstrated that in the case of a finite FSS phonons can reduce the degree of entanglement by increasing dephasing and assisting off-resonant single-photon transitions [32]. In view of all the above-mentioned different ways how phonons may affect the degree of entanglement generated in an exciton-biexciton system, it is unclear – without further investigations – what role phonons may play when combined with the effects introduced by the finite pulse duration needed for TPE preparation of the system in the biexciton state.

In this work, we investigate the combined impact of the TPE scheme and LA phonons on polarization-entangled photon pairs emitted by strongly-confining GaAs-based quantum dots. Section II specifies the theoretical model for the optically excited QD as well as the calculation scheme for the two-photon density matrix and the degree of entanglement. Based on this model, the degree of entanglement, as measured by the concurrence, is studied as a function of temperature and pulse duration in Section III. Indeed, it is found that the combination of TPE and the coupling to LA phonons results in an additional decrease of the concurrence. For practical applications it is equally important to know how this additional drop depends on temperature. This is not only relevant at cryogenic temperatures that are usually used in attempts to maximize the degree of entanglement. While at such low temperatures one usually wants to know what limit is set by phonons to the maximum level of entanglement, at higher temperatures the focus shifts to the question of whether there is still enough entanglement left to realize a useful source of entangled photons at temperatures that are more convenient for practicable applications. We have therefore determined the temperature dependence of the concurrence up to more elevated temperatures and find a decreasing concurrence with rising temperature, even if the FSS vanishes. Furthermore, this detrimental effect increases with rising pulse duration. However, we find that at 50 K the emitted photons can still be entangled to 90% indicating promising perspectives for applications at elevated temperatures.

II. THEORETICAL MODEL AND EVALUATION OF ENTANGLEMENT

We consider a strongly-confining InGaAs QD coupled to a continuum of LA phonons that is optically excited using the TPE scheme, as schematically illustrated in Figure 1. The biexciton is excited with a Gaussian laser pulse that is tuned to the two-photon resonance. Due to the strong confinement, higher excited states can be neglected and the QD is modeled as a four-level system. In the ideal situation, the decay of the biexciton yields the maximally entangled state $|\Phi_+\rangle$ described by the ideal two-photon density matrix shown in the lower right corner of Figure 1.

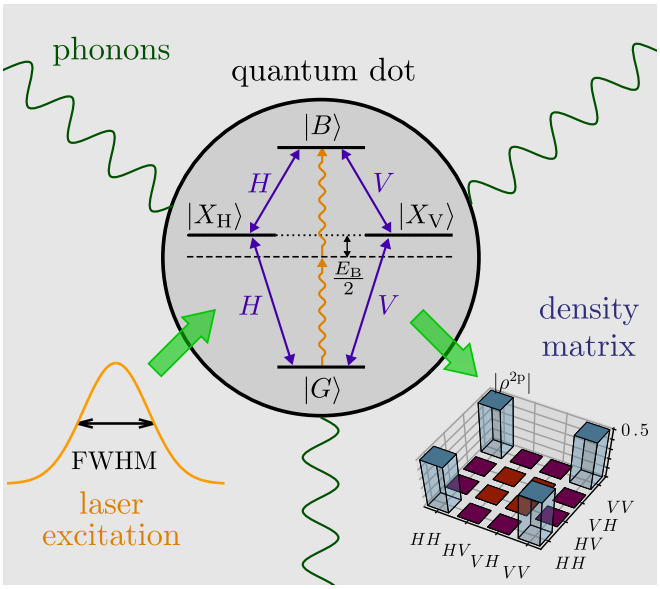

FIG. 1. Sketch of the considered system. In the two-photon excitation scheme, a Gaussian laser pulse (left) with finite full-width-at-half-maximum (FWHM) is tuned to the two-photon resonance of a semiconductor quantum dot (center). Furthermore, due to its environment, the quantum dot is coupled to longitudinal acoustic phonons. The excited biexciton decays radiatively, following the biexciton-exciton cascade. In the ideal situation, either two horizontally (H) or two vertically (V) polarized photons are emitted, resulting in the creation of the maximally entangled state $|\Phi_+\rangle$, as described by the ideal two-photon density matrix $\rho^{2\mathrm{p}}$ (right).

A. Optically excited strongly-confining quantum dots

The electronic structure of the QD is modeled as a four-level system, comprising the electronic ground state $|G\rangle$, two exciton states $|X_{\mathrm{H/V}}\rangle$ that couple to horizontally and vertically polarized light, respectively, and the biexciton state $|B\rangle$. In the frame co-rotating with the external laser frequency ω_L, the corresponding Hamiltonian is given by

$$\hat{H}_\mathrm{QD} = \left(\Delta_\mathrm{XL} + \frac{\delta}{2}\right)|X_\mathrm{H}\rangle\langle X_\mathrm{H}| + \left(\Delta_\mathrm{XL} - \frac{\delta}{2}\right)|X_\mathrm{V}\rangle\langle X_\mathrm{V}| + (2\Delta_\mathrm{XL} - E_\mathrm{B})\,|B\rangle\langle B|, \tag{2}$$

where the energy of the ground state is used as the zero of the energy scale. Here $\Delta_\mathrm{XL} := \hbar\,(\omega_\mathrm{X} - \omega_\mathrm{L})$ is the de-

tuning between the mean exciton energy $\hbar\omega_{\mathrm{X}}$ and the excitation laser, δ is the FSS, and E_{B} denotes the biexciton binding energy.

In the TPE scheme, the biexciton is directly excited with a short laser pulse tuned to the two-photon transition energy, i.e., $\Delta_{\mathrm{XL}} = E_{\mathrm{B}}/2$. We assume a Gaussian pulse shape with envelope function

$$\Omega(t) = \sqrt{\frac{4\ln(2)}{\pi}}\frac{\Theta}{\Delta_{\mathrm{FWHM}}}\exp\left[-4\ln(2)\left(\frac{t-t_{\mathrm{L}}}{\Delta_{\mathrm{FWHM}}}\right)^2\right], \tag{3}$$

where the pulse duration is characterized by the full-width-at-half-maximum (FWHM) Δ_{FWHM}. In typical experiments, the pulse duration is around 10 ps [3, 23, 25]. Note that the FWHM of the corresponding intensity profile $I(t) \propto \Omega^2(t)$ is $\Delta_{\mathrm{FWHM}}/\sqrt{2}$. t_{L} denotes the time of the pulse maximum and Θ is the (one-photon) pulse area. In the rotating wave approximation, the interaction between the QD and the laser pulse is described by the Hamiltonian

$$\hat{H}_{\mathrm{L}} = \Omega(t)\left(\hat{\sigma}_{\mathrm{L}} + \hat{\sigma}_{\mathrm{L}}^{\dagger}\right), \tag{4}$$

where the linear polarization of the laser is encoded in the coefficients $\alpha_{\mathrm{H/V}} \in \mathbb{R}$ in the operator

$$\hat{\sigma}_{\mathrm{L}} = \alpha_{\mathrm{H}}\hat{\sigma}_{\mathrm{H}} + \alpha_{\mathrm{V}}\hat{\sigma}_{\mathrm{V}}. \tag{5}$$

Here the operator $\hat{\sigma}_{\mathrm{H/V}} := |G\rangle\langle X_{\mathrm{H/V}}| + |X_{\mathrm{H/V}}\rangle\langle B|$ describes the QD transitions coupled to horizontally/vertically polarized light. In this work, two different (linear) laser polarizations are considered: (i) horizontal laser polarization, i.e., $\alpha_{\mathrm{H}} = 1$, $\alpha_{\mathrm{V}} = 0$, and (ii) diagonal laser polarization, i.e., $\alpha_{\mathrm{H}} = \alpha_{\mathrm{V}} = 1/\sqrt{2}$, with equal components in H and V direction.

The transitions between QD states that result in photon emission are modeled as radiative decay processes. They are described by Lindblad operators [46]

$$\mathcal{L}_{\hat{O},\Gamma}\hat{\rho} = \frac{\Gamma}{2}\left(2\hat{O}\hat{\rho}\hat{O}^{\dagger} - \hat{O}^{\dagger}\hat{O}\hat{\rho} - \hat{\rho}\hat{O}^{\dagger}\hat{O}\right) \tag{6}$$

with the corresponding transition operator $\hat{O}$ and rate Γ, that act on the statistical operator of the system $\hat{\rho}$. Due to the optical selection rules, the possible radiative decay processes are described by the four operators: $\mathcal{L}_{|G\rangle\langle X_{\mathrm{H}}|,\gamma_{\mathrm{X}}}$, $\mathcal{L}_{|G\rangle\langle X_{\mathrm{V}}|,\gamma_{\mathrm{X}}}$, $\mathcal{L}_{|X_{\mathrm{H}}\rangle\langle B|,\frac{\gamma_{\mathrm{B}}}{2}}$, and $\mathcal{L}_{|X_{\mathrm{V}}\rangle\langle B|,\frac{\gamma_{\mathrm{B}}}{2}}$. Here, γ_{B} (γ_{X}) is the radiative decay rate of the biexciton (an exciton) state.

In strongly-confining InGaAs QDs, the most important electron-phonon interaction at low temperatures is the deformation potential coupling to a continuum of LA phonons [47–50]. This coupling is of the pure dephasing type and is described by the Hamiltonian

$$\hat{H}_{\mathrm{Ph}} = \hbar\sum_{\mathbf{q}}\omega_{\mathbf{q}}\hat{b}_{\mathbf{q}}^{\dagger}\hat{b}_{\mathbf{q}} + \hbar\sum_{\chi,\mathbf{q}} n_{\chi}\left(\gamma_{\mathbf{q}}^{\mathrm{X}}\hat{b}_{\mathbf{q}}^{\dagger} + \gamma_{\mathbf{q}}^{\mathrm{X}*}\hat{b}_{\mathbf{q}}\right)|\chi\rangle\langle\chi|, \tag{7}$$

where the bosonic operator $\hat{b}_{\mathbf{q}}^{\dagger}$ creates a phonon in mode $\mathbf{q}$ with energy $\hbar\omega_{\mathbf{q}}$, $n_{\chi} = \{0,1,1,2\}$ denotes the number of excitons present in the QD state $|\chi\rangle = \{|G\rangle, |X_{\mathrm{H}}\rangle, |X_{\mathrm{V}}\rangle, |B\rangle\}$, and $\gamma_{\mathbf{q}}^{\mathrm{X}}$ is the exciton-phonon coupling strength. Here, we have classified the above exciton-phonon coupling as being of *pure dephasing type* since the coupling is only to the occupations of the states $|\chi\rangle$ and not to transitions between them. It should be noted that combining such a pure dephasing type coupling with other interactions, the pure dephasing coupling may also affect the dynamics of the occupations as is manifested, e.g., in the damping of Rabi oscillations [51–54].

The dynamics of the statistical operator $\hat{\rho}$ of the complete system is governed by the Liouville-von Neumann equation

$$\frac{\mathrm{d}}{\mathrm{d}t}\hat{\rho} = -\frac{i}{\hbar}\left[\hat{H},\hat{\rho}\right] + \sum_{\ell=H,V}\left\{\mathcal{L}_{|G\rangle\langle X_{\ell}|,\gamma_{\mathrm{X}}} + \mathcal{L}_{|X_{\ell}\rangle\langle B|,\frac{\gamma_{\mathrm{B}}}{2}}\right\}\hat{\rho} \tag{8}$$

$$\hat{H} = \hat{H}_{\mathrm{QD}} + \hat{H}_{\mathrm{L}} + \hat{H}_{\mathrm{Ph}}, \tag{9}$$

where $[\hat{A},\hat{B}]$ is the commutator of two operators $\hat{A}$ and $\hat{B}$. Employing a numerically complete real-time path-integral method detailed in Refs. 55–59, the dynamics of the reduced QD density matrix $\hat{\tilde{\rho}} = \mathrm{Tr}_{\mathrm{Ph}}\{\hat{\rho}\}$ is obtained. In the path-integral algorithm, the coupling to LA phonons enters via the phonon spectral density $J(\omega) = \sum_{\mathbf{q}}|\gamma_{\mathbf{q}}^{\mathrm{X}}|^2\delta(\omega-\omega_{\mathbf{q}})$. An explicit expression for this quantity can be found in Ref. 58 and the necessary GaAs material parameters are taken from Ref. 49. In this work, we consider a spherically symmetric InGaAs QD with a harmonic confinement and electron (hole) confinement length $a_e = 3$ nm ($a_h = a_e/1.15$). Furthermore, we use realistic parameters for the remaining QD properties, listed in Table I. For our numerical simulations, we assume that the phonons are initially in a thermal equilibrium at temperature T, while the QD is in its ground state $|G\rangle$. Note that for each simulation the optimal pulse area Θ is determined numerically by optimizing for the maximum biexciton occupation after the pulse.

The numerical completeness of our simulation means that, in order to evaluate the dynamical variables of interest, no approximations to the model are made. We are neither using an expansion with respect to a presumably small parameter such as the exciton-phonon or exciton-laser coupling nor do we neglect memory effects as done by Markovian approaches. In particular, the memory functions representing the phonon-induced memory can be evaluated beforehand [57, 59] such that the depth of the memory is known before starting the path-integral simulation. Numerical errors arise in our simulation only due to discretization errors that are easily checked for convergence.

TABLE I. Realistic quantum dot parameters.

Parameter		Value
Biexciton binding energy	E_{B}	4 meV
Exciton-laser detuning	Δ_{XL}	$E_{\mathrm{B}}/2 = 2$ meV
Radiative decay rate exciton	γ_{X}	0.005 ps^{-1}
Radiative decay rate biexciton	γ_{B}	$2\gamma_{\mathrm{X}} = 0.010$ ps^{-1}

B. Reconstructed photonic density matrix and concurrence

State-of-the-art experiments employ quantum state tomography [60] to reconstruct the emitted two-photon state. This measurement scheme is based on polarization-resolved two-time coincidence measurements. The obtained signals are proportional to two-time correlation functions of photon operators. Because the sources of the emitted photons are electronic transitions between the QD states, i.e., the radiative decay, the two-time correlation function can be calculated using QD state transition operators as

$$G^{(2)}_{jk,\ell m}(t,\tau) = \left\langle \hat{\sigma}^{\dagger}_{j}(t)\hat{\sigma}^{\dagger}_{k}(t+\tau)\hat{\sigma}_{m}(t+\tau)\hat{\sigma}_{\ell}(t)\right\rangle, \quad (10)$$

where $\{j,k,\ell,m\} \in \{H,V\}$. Here, t denotes the time of the first photon detection event, while τ is the delay time until a subsequent second one occurs.

In experiments, one always measures quantities averaged over finite real time and delay time windows. Usually, the average interval for the real time T_{av} is chosen such that it encompasses the complete decay process. However, different subsets of emitted photons can be selected choosing different delay time windows τ_{av} [31]. While a shorter delay time window is typically advantageous for the degree of entanglement [31, 61, 62], the corresponding photon yield is reduced. Since, however, in applications often a high yield is mandatory, all created photons should be utilized. Thus, we aim for the maximum photon yield and consider all photon emission events. Consequently, we calculate the two-photon density matrix $\rho^{2\mathrm{p}}$ as

$$\rho^{2\mathrm{p}}_{jk,\ell m} = \frac{\overline{G}^{(2)}_{jk,\ell m}}{\mathrm{Tr}\left\{\overline{G}^{(2)}\right\}}, \quad (11)$$

$$\overline{G}^{(2)}_{jk,\ell m} = \lim_{T_{\mathrm{av}},\tau_{\mathrm{av}}\to\infty} \int_0^{T_{\mathrm{av}}} \mathrm{d}t \int_0^{\tau_{\mathrm{av}}} \mathrm{d}\tau\, G^{(2)}_{jk,\ell m}(t,\tau), \quad (12)$$

where both time windows are taken in the limit of infinity. Details on the numerical evaluation of two-time correlation functions within the path-integral formalism can be found in Ref. 63. It is important to note that our approach avoids using the quantum regression theorem (QRT). The QRT is the standard tool for evaluating two-time correlation functions. However, its derivation relies on the assumption that all environment influences are Markovian [64, 65], which is not true for phonons. Using the QRT naively in the bare state basis yields emission spectra where the phonon sidebands appear energetically on the wrong side [66]. Working in a polaron transformed frame by using the polaron master equations (PMEs) the correct energetic position of the sidebands is recovered [67–69]. However, even an advanced scheme like the PME, which works very well for single-time density matrices and captures many of the pertinent non-Markovian features of emission spectra, turns out to yield noticeable errors in evaluating two-time correlation functions needed, e.g., for the indistinguishability [70]. Using a numerically complete scheme we are on the safe side to obtain correct values for the two-time correlation functions required for our present study.

The degree of entanglement associated with a reconstructed two-photon density matrix is quantified using the concurrence, a well-established entanglement measure that has a one-to-one correspondence to the entanglement of formation [71, 72]. In the basis $\{|HH\rangle, |HV\rangle, |VH\rangle, |VV\rangle\}$, the concurrence C is obtained directly from the two-photon density matrix

$$C = \max\left\{0, \sqrt{\lambda_1} - \sqrt{\lambda_2} - \sqrt{\lambda_3} - \sqrt{\lambda_4}\right\}, \quad (13)$$

where $\lambda_j \geq \lambda_{j+1}$ are the (real and positive) eigenvalues of the 4×4-matrix

$$M = \rho^{2\mathrm{p}}\,\Sigma\,(\rho^{2\mathrm{p}})^{*}\,\Sigma\,. \quad (14)$$

Here, Σ is the anti-diagonal matrix with elements $\{-1,1,1,-1\}$ and $(\rho^{2\mathrm{p}})^{*}$ denotes the complex conjugated two-photon density matrix.

III. PHONON INFLUENCE DURING TWO-PHOTON EXCITATION

The focus of this work is to investigate the combined impact of the TPE scheme and the pure dephasing-type coupling to LA phonons on the degree of entanglement of photon pairs emitted from strongly-confining QDs. First, the influence of phonons on the two-photon state is analyzed for a typical fixed pulse duration. Afterward, we study the combined impact for varying lengths of the excitation pulse.

A. Temperature-dependent degradation of the entanglement

We consider a typical pulse duration of $\Delta_{\mathrm{FWHM}} = 10$ ps [3, 23, 25] and investigate the temperature dependence of the obtained concurrence. Figure 2(a) displays the concurrence as a function of temperature T for horizontal (H, filled symbols) and diagonal (D, open symbols) laser polarization. A vanishing FSS (blue) as well as

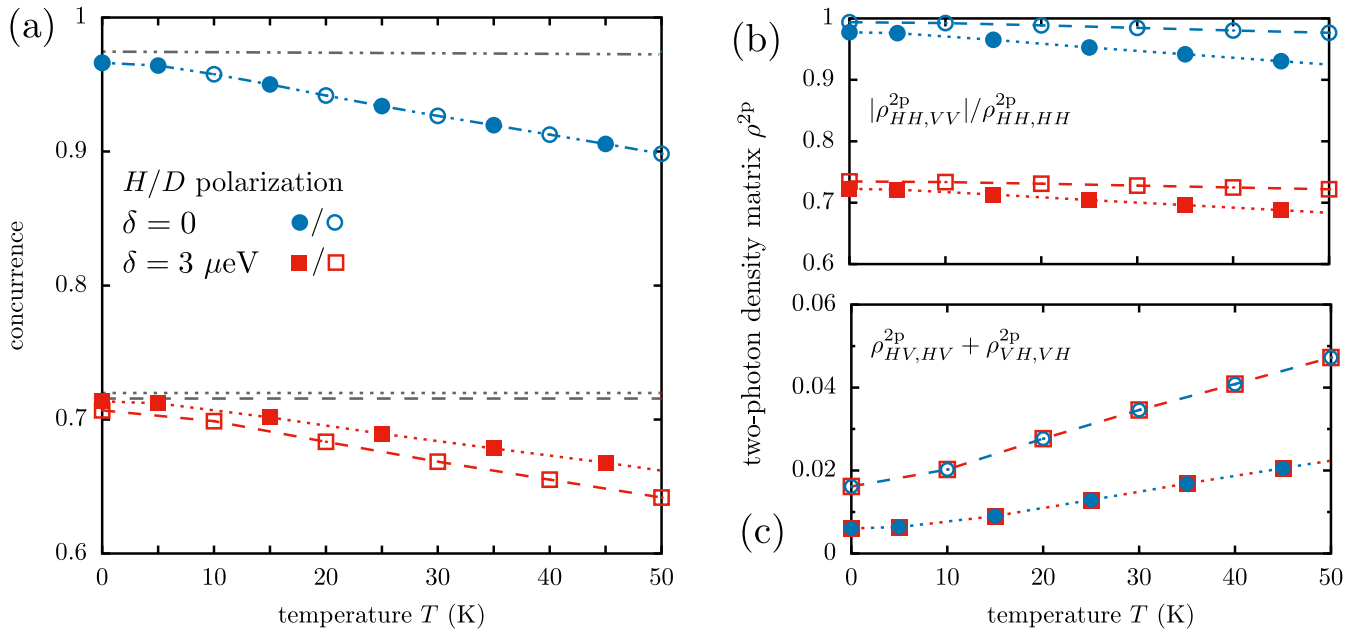

FIG. 2. (a) Concurrence as a function of temperature for a typical pulse duration $\Delta_{\mathrm{FWHM}} = 10$ ps. Two different laser polarizations [horizontal (H): filled symbols and diagonal (D): open symbols] as well as two fine-structure splittings $\delta = 0$ (blue circles) and 3 μeV (red squares) are considered. The symbols represent numerical results and dotted (dashed) lines indicate a guide to the eye for horizontal (diagonal) laser polarization. The corresponding phonon-free results are indicated by gray horizontal lines with the same dash type. For $\delta = 0$, the results for H and D polarization are exactly the same. (b) Ratio between the two-photon density matrix elements $|\rho^{2\mathrm{p}}_{HH,VV}|$ and $\rho^{2\mathrm{p}}_{HH,HH}$, and (c) sum of the elements $\rho^{2\mathrm{p}}_{HV,HV}$ and $\rho^{2\mathrm{p}}_{VH,VH}$ for the calculations presented in panel (a).

a finite FSS of $\delta = 3$ μeV (red) is considered. In all cases, the degree of entanglement decreases monotonically with rising temperature, revealing a phonon-induced degradation of the entanglement. While the obtained concurrence is independent of the laser polarization for a vanishing FSS, the difference ΔC between the concurrence obtained for horizontal and diagonal laser polarization increases with temperature when the FSS is finite. Although the concurrence comes close to the corresponding phonon-free result (gray horizontal lines) in the limit $T \to 0$, the latter is not recovered, even for $T = 0$.

In order to understand the phonon influence, we briefly recapitulate the results for an ideal four-level quantum emitter, i.e., the phonon-free case, discussed in Ref. 40. It was found that the degree of entanglement is limited due to a laser-induced which-path information introduced during the excitation pulse; cf. gray horizontal lines in Figure 2(a). Because there is a finite probability that the biexciton decays into an exciton state already during the pulse, this which-path information impacts the emitted two-photon state and reduces the concurrence. Note that reexcitation is hardly a factor in the phonon-free case since the one-photon process bringing the QD from the exciton state back into the biexciton is strongly detuned from the laser energy. In the polarization basis $\{H, V\}$, the laser-induced which-path information is interpreted differently, depending on the chosen laser polarization. In the case of the horizontal laser polarization, an energy splitting on the order of $E_{\mathrm{S}} \sim \hbar\pi/\Delta_{\mathrm{FWHM}}$ is introduced between the two exciton states $|X_{\mathrm{H}}\rangle$ and $|X_{\mathrm{V}}\rangle$ due to the AC Stark effect. Similar to the FSS, the splitting E_{S} results in dephasing and a reduced coherence $\rho^{2\mathrm{p}}_{HH,VV}$ in the two-photon density matrix. On the other hand, a diagonal laser polarization introduces an effective coupling between these exciton states, creating undesired photon states $|HV\rangle$ and $|VH\rangle$. Because all linear laser polarizations are equivalent, in the case of a vanishing FSS, the resulting concurrence is exactly the same for both laser polarizations. However, if the FSS is finite, using a horizontal laser polarization gives a slightly higher concurrence.

Similar to the phonon-free case, the phonon effects that reduce the degree of entanglement depend on the laser polarization. We start the analysis with the case of the horizontal laser polarization. In this situation, the loss of entanglement can be traced back to two phonon-related effects. The laser couples only to QD transitions involving $|X_{\mathrm{H}}\rangle$ and, thus, introduces an effective splitting E_{S} between the exciton states. Because the exciton states are energetically split during the pulse, phonons can reduce the concurrence by increasing dephasing [32]. Due to the effective splitting the two decay paths are associated with different transition energies. Thus, phonons enlarge the which-path information as energies of involved phonons depend on the decay path. This enlarged which-path information results in phonon-enhanced dephasing

and a reduced coherence between the two-photon states $|HH\rangle$ and $|VV\rangle$; cf. filled symbols in Figure 2(b). When the temperature increases, more phonons become thermally excited. Thus, the phonon-induced dephasing is the stronger the higher the temperature, and the corresponding coherence $\rho^{\mathrm{2p}}_{HH,VV}$ and concurrence decrease with rising T.

In addition, the interaction with LA phonons also increases the reexcitation probability. Phonon absorption and emission processes can assist the off-resonant single-photon processes by compensating the energy mismatch between the QD transition energies and the energy of the laser [32]. Thus, when the biexciton decays into the exciton state $|X_{\mathrm{H}}\rangle$, under emission of a H polarized photon, already during the pulse, a reexcitation of the biexciton state induced by the same laser pulse becomes more likely since a phonon with the energy covering the detuning can be emitted. Because the biexciton can now again decay into either exciton state, the undesired state $|HV\rangle$ can be created, which also reduces the degree of entanglement. Also the probabilities of phonon absorption and emission processes increase with rising temperature. Consequently, phonon-assisted reexcitation processes are more likely to occur at higher temperatures. This effect can be seen in Figure 2(c), which shows an increasing probability to find a detrimental two-photon state $\rho^{\mathrm{2p}}_{HV,HV}+\rho^{\mathrm{2p}}_{VH,VH}$ with rising temperature; cf. filled symbols. Note that for a horizontal laser polarization, $|X_{\mathrm{V}}\rangle$ is decoupled from the laser excitation. Thus, two-photon states $|VH\rangle$ are insignificant, i.e., $\rho^{\mathrm{2p}}_{HV,HV} \gg \rho^{\mathrm{2p}}_{VH,VH}$ (not shown). Because both phonon-related effects that degrade the entanglement – the phonon-induced dephasing and the phonon-assisted reexcitation – increase with temperature, the resulting concurrence decreases monotonically as a function of T. Note that the phonon-free result (gray horizontal line) is not recovered for $T = 0$ because phonon emission processes are still possible. Furthermore, because typical FSSs are much smaller than the energy mismatch between the laser and QD transition energies, i.e., $\delta \ll E_{\mathrm{B}}/2$, the energy of phonons that needs to be absorbed or emitted hardly changes. Thus, the associated reexcitation probability, and hence $\rho^{\mathrm{2p}}_{HV,HV} + \rho^{\mathrm{2p}}_{VH,VH}$, remain the same when considering a finite FSS $\delta = 3$ μeV; cf. red and blue symbols in Figure 2(c).

Next, we turn to a diagonal laser polarization. In this situation, the phonon-related mechanism that causes the degradation of entanglement with rising T is slightly different. Essentially, only one of the two effects discussed above, i.e., phonon-assisted reexcitation, is relevant here. For a diagonal laser polarization, the TPE scheme introduces an effective coupling between the exciton states $|X_{\mathrm{H}}\rangle$ and $|X_{\mathrm{V}}\rangle$, rather than an energy splitting. Therefore, the phonon-induced dephasing is marginal and the relative coherence $\rho^{\mathrm{2p}}_{HH,VV}$ is hardly reduced; cf. open symbols in Figure 2(b). On the other hand, both exciton states are coupled to the laser excitation. Consequently, phonon-assisted reexcitation leads to a much higher probability to obtain detrimental two-photon states; cf. open symbols in Figure 2(c). Note that for a diagonal laser polarization the system is symmetric with respect to H and V polarization. Thus, the probability to find mixed two-photon states $|HV\rangle$ and $|VH\rangle$ is equal, i.e., $\rho^{\mathrm{2p}}_{HV,HV} = \rho^{\mathrm{2p}}_{VH,VH}$ (not shown).

For a vanishing FSS, no linear polarization basis is distinguished, even when the coupling to phonons is present. Thus, from a physical point of view, the concurrence has to be independent of the chosen (linear) laser polarization. Indeed, the concurrence for horizontal and diagonal laser polarization is exactly the same; cf. blue symbols in Figure 2(a). But, for a fixed polarization basis, the weights of the two phonon effects depend on the chosen laser polarization. Thus, the phonon impact on elements of the two-photon density matrix differs for horizontal and diagonal laser polarization; cf. panels (b) and (c). However, for vanishing FSS, both cases describe the same physical situation, just from a different perspective. Consequently, the two different two-photon density matrices obtained for horizontal and diagonal laser polarization are linked by a simple basis transformation. This means, when one transforms the polarization basis from H and V polarization to the diagonal $D = (H + V)/\sqrt{2}$ and anti-diagonal $A = (H - V)/\sqrt{2}$ basis, the two different density matrices are precisely converted into each other.

However, when the FSS is finite the basis $\{H, V\}$ is distinguished and the concurrence depends on the chosen laser polarization. As in the phonon-free case, the horizontal laser polarization gives a higher concurrence compared to a diagonal one. Furthermore, the difference in concurrence ΔC is enlarged by the interaction with LA phonons and increases with temperature.

B. Increasing phonon impact for longer pulses

After the origins for the observed temperature-dependent degradation of entanglement have been identified to be phonon-induced dephasing and phonon-assisted reexcitation, we now investigate the concurrence as a function of the pulse duration. Although the laser-induced splitting or coupling between the exciton states decreases with rising pulse duration (because the pulse peak intensity is decreased when the pulse area is kept fixed), more emission events are impacted by the laser-induced effects when the pulse becomes longer. Consequently, already in the phonon-free case, the achievable degree of entanglement drops with rising FWHM [40]. In addition, also the detrimental phonon-related effects have more time to impact the system when the pulse duration is increased. Consequently, at a given temperature, the concurrence should decrease for longer pulses. Furthermore, the drop in concurrence with increasing temperature should be the stronger the longer the pulse duration is.

The numerical results presented in Figure 3 confirm these expectations. For a given temperature, the concur-

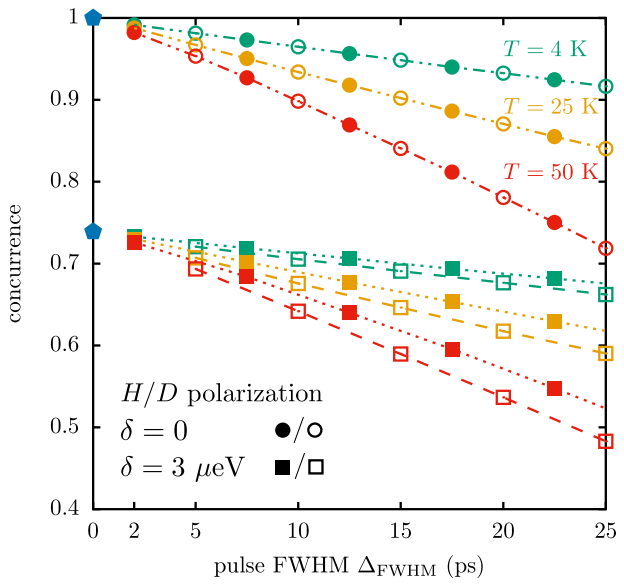

FIG. 3. Concurrence in dependence of the pulse duration, characterized by its FWHM, for two laser polarizations [horizontal (H): filled symbols and diagonal (D): open symbols] and two fine-structure splittings: $\delta = 0$ (circles) and 3 μeV (squares). Three different temperatures are considered: $T = 4$ K (green), 25 K (orange), and 50 K (red). The symbols represent numerical results and dotted (dashed) lines indicate a guide to the eye for horizontal (diagonal) laser polarization. For $\delta = 0$, the results for H and D polarization are exactly the same. Data points at $\Delta_{\mathrm{FWHM}} = 0$ (blue pentagons) represent phonon-free calculations for an initially prepared biexciton without optical excitation.

rence decreases monotonically when the pulse duration is increased. Furthermore, the slope of this decrease steepens with rising FWHM. Thus, both phonon-related mechanisms, indeed, become more relevant for longer pulses. For a vanishing FSS, all linear laser polarizations are equivalent, resulting again in exactly the same concurrence for horizontal and diagonal polarization. Because the phonon-related effects are more important at higher temperatures and/or longer pulse durations, the difference in concurrence between the two laser polarizations found for a finite FSS $\delta = 3$ μeV increases as well.

In the limit of $\Delta_{\mathrm{FWHM}} \to 0$ the combined, detrimental effect of TPE and LA phonons fades away, and the corresponding concurrence approaches the phonon-free result for an initially prepared biexciton, indicated by blue pentagons in Figure 3. In this sense it is indeed the finite pulse duration that unlocks the phonon impact on the concurrence. However, one has to keep in mind that the TPE scheme breaks down in this limit. For a typical GaAs-based QD, a pulse duration below $\lesssim 3$ ps results in a strongly reduced preparation probability of the biexciton, because the energy spectrum of the laser pulse begins to overlap with the exciton transition energies [73]. Thus, below these pulse durations, the concurrence can only be enhanced if one is willing to accept a severe decline in the photon yield. Note that the reduced probability to excite the biexciton does not reduce the concurrence, because the coincidence measurements only consider cases where two photons are emitted.

IV. CONCLUSION

We have investigated the combined impact of TPE and the pure dephasing-type coupling to LA phonons on the achievable entanglement of photon pairs emitted from strongly-confining QDs. It is found that the interaction with phonons reduces the degree of entanglement, as measured by the concurrence, further below the recently established limitation due to the TPE scheme itself. At a fixed pulse duration, the combined impact results in a monotonic decrease of the concurrence when the temperature increases. This phonon-induced degradation of the entanglement does not vanish in the limit of vanishing temperature. Depending on the chosen laser polarization, the origin of this temperature-dependent degradation is found to be a combination of phonon-induced dephasing and phonon-assisted one-photon processes that increase the probability to find the mixed states $|HV\rangle$ and $|VH\rangle$ after reexcitation of the biexciton.

Because phonons have more time to influence the system for longer pulses the degree of entanglement decreases with rising temperature and/or pulse duration, even in the absence of an excitonic fine-structure splitting. Furthermore, when the fine-structure splitting is finite, the coupling to phonons enlarges the difference in concurrence obtained for different laser polarizations that is already present in the phonon-free case. Although the combined, detrimental impact of TPE and LA phonons disappears in the limit of zero pulse duration and vanishing FSS, the TPE scheme in QDs typically breaks down below a FWHM of $\Delta_{\mathrm{FWHM}} \lesssim 3$ ps. Hence, in realistic situations, one will always observe a temperature-dependent degradation of entanglement for photon pairs emitted by a strongly-confining QD.

Finally, we would like to mention that a temperature-dependent drop of the concurrence has recently also been observed in the case of vanishing FSS for QDs that are not in the strong-confinement limit [74]. For these larger quantum dots, the pure dephasing-like coupling to phonons becomes negligible because the effective coupling strength decreases with rising QD size [75, 76]. However, the phonon-mediated coupling to higher energetic states has been identified in that study as the origin of the reduction in concurrence. For strongly-confining QDs, we are dealing here with the reverse situation where couplings to higher energetic states are negligible but pure dephasing becomes important. Indeed, in our present study, we demonstrate a noticeable degradation of the concurrence even when higher states are completely absent. Interestingly, the temperature dependence observed in Ref. 74 differs from our present result: there the concurrence stays on a plateau for lower tem-

peratures before it drops much more steeply than found in the present paper. Indeed, while we find in Fig. 2(a) for $\delta = 0$ and $T = 50$ K a concurrence that is still $\sim$0.9, for the larger QDs in Ref. 74 the corresponding value was almost reduced to 0.4. Thus, we see a clear advantage of strongly-confining QDs at elevated temperatures. On the other hand, strongly-confining QDs are usually characterized by smaller optical transition rates, which make these systems more vulnerable to residual FSS and other noise sources. A holistic treatment of QD excitonic structure and excitation scheme, and a detailed knowledge of dephasing and reexcitation sources will thus be needed to create QDs capable of generating maximally entangled photons at elevated temperatures.

ACKNOWLEDGMENTS

T. K. B. and D. E. R. acknowledge support by the Deutsche Forschungsgemeinschaft (DFG) via the project No. 428026575. A. R. acknowledges financial support by the Austrian Science Fund (FWF) via the Research Group FG5, P 29603, P 30459, I 4320, I 4380, I 3762, the European Union's Horizon 2020 research and innovation program under Grant Agreements No. 899814 (Qurope) and No. 871130 (Ascent+), the QuantERA II Programme that has received funding from the European Union's Horizon 2020 research and innovation program under Grant Agreement No. 101017733 via the project QD-E-QKD and the FFG Grant No. 891366, the Linz Institute of Technology (LIT), and the LIT Secure and Correct Systems Lab, supported by the State of Upper Austria. We are further grateful for support by the Deutsche Forschungsgemeinschaft (DFG, German Research Foundation) via the project No. 419036043.

[1] N. Gisin, G. Ribordy, W. Tittel, and H. Zbinden, Quantum cryptography, Rev. Mod. Phys. **74**, 145 (2002).
[2] H.-K. Lo, M. Curty, and K. Tamaki, Secure quantum key distribution, Nat. Photonics **8**, 595 (2014).
[3] C. Schimpf, M. Reindl, D. Huber, B. Lehner, S. F. Covre Da Silva, S. Manna, M. Vyvlecka, P. Walther, and A. Rastelli, Quantum cryptography with highly entangled photons from semiconductor quantum dots, Sci. Adv. **7**, eabe8905 (2021).
[4] F. Basso Basset, M. Valeri, E. Roccia, V. Muredda, D. Poderini, J. Neuwirth, N. Spagnolo, M. B. Rota, G. Carvacho, F. Sciarrino, and R. Trotta, Quantum key distribution with entangled photons generated on demand by a quantum dot, Sci. Adv. **7**, eabe6379 (2021).
[5] L.-M. Duan, M. D. Lukin, J. I. Cirac, and P. Zoller, Long-distance quantum communication with atomic ensembles and linear optics, Nature **414**, 413 (2001).
[6] J.-W. Pan, Z.-B. Chen, C.-Y. Lu, H. Weinfurter, A. Zeilinger, and M. Żukowski, Multiphoton entanglement and interferometry, Rev. Mod. Phys. **84**, 777 (2012).
[7] C. H. Bennett and D. P. DiVincenzo, Quantum information and computation, Nature **404**, 247 (2000).
[8] S. C. Kuhn, A. Knorr, S. Reitzenstein, and M. Richter, Cavity assisted emission of single, paired and heralded photons from a single quantum dot device, Opt. Express **24**, 25446 (2016).
[9] A. Zeilinger, Light for the quantum. Entangled photons and their applications: a very personal perspective, Phys. Scr. **92**, 072501 (2017).
[10] A. Orieux, M. A. M. Versteegh, K. D. Jöns, and S. Ducci, Semiconductor devices for entangled photon pair generation: a review, Rep. Prog. Phys. **80**, 076001 (2017).
[11] O. Benson, C. Santori, M. Pelton, and Y. Yamamoto, Regulated and Entangled Photons from a Single Quantum Dot, Phys. Rev. Lett. **84**, 2513 (2000).
[12] R. M. Stevenson, R. J. Young, P. Atkinson, K. Cooper, D. A. Ritchie, and A. J. Shields, A semiconductor source of triggered entangled photon pairs, Nature **439**, 179 (2006).
[13] R. J. Young, R. M. Stevenson, P. Atkinson, K. Cooper, D. A. Ritchie, and A. J. Shields, Improved fidelity of triggered entangled photons from single quantum dots, New J. Phys. **8**, 29 (2006).
[14] R. Hafenbrak, S. M. Ulrich, P. Michler, L. Wang, A. Rastelli, and O. G. Schmidt, Triggered polarization-entangled photon pairs from a single quantum dot up to 30 K, New J. Phys. **9**, 315 (2007).
[15] A. Muller, W. Fang, J. Lawall, and G. S. Solomon, Creating Polarization-Entangled Photon Pairs from a Semiconductor Quantum Dot Using the Optical Stark Effect, Phys. Rev. Lett. **103**, 217402 (2009).
[16] A. Dousse, J. Suffczyński, A. Beveratos, O. Krebs, A. Lemaître, I. Sagnes, J. Bloch, P. Voisin, and P. Senellart, Ultrabright source of entangled photon pairs, Nature **466**, 217 (2010).
[17] A. J. Bennett, M. A. Pooley, R. M. Stevenson, M. B. Ward, R. B. Patel, A. Boyer de la Giroday, N. Sköld, I. Farrer, C. A. Nicoll, D. A. Ritchie, and A. J. Shields, Electric-field-induced coherent coupling of the exciton states in a single quantum dot, Nat. Phys. **6**, 947 (2010).
[18] R. M. Stevenson, C. L. Salter, J. Nilsson, A. J. Bennett, M. B. Ward, I. Farrer, D. A. Ritchie, and A. J. Shields, Indistinguishable Entangled Photons Generated by a Light-Emitting Diode, Phys. Rev. Lett. **108**, 040503 (2012).
[19] M. Müller, S. Bounouar, K. D. Jöns, M. Glässl, and P. Michler, On-demand generation of indistinguishable polarization-entangled photon pairs, Nat. Photonics **8**, 224 (2014).
[20] R. Trotta, J. S. Wildmann, E. Zallo, O. G. Schmidt, and A. Rastelli, Highly Entangled Photons from Hybrid Piezoelectric-Semiconductor Quantum Dot Devices, Nano Lett. **14**, 3439 (2014).
[21] R. Winik, D. Cogan, Y. Don, I. Schwartz, L. Gantz, E. R. Schmidgall, N. Livneh, R. Rapaport, E. Buks, and D. Gershoni, On-demand source of maximally entangled

photon pairs using the biexciton-exciton radiative cascade, Phys. Rev. B **95**, 235435 (2017).
[22] D. Huber, M. Reindl, Y. Huo, H. Huang, J. S. Wildmann, O. G. Schmidt, A. Rastelli, and R. Trotta, Highly indistinguishable and strongly entangled photons from symmetric GaAs quantum dots, Nat. Commun. **8**, 15506 (2017).
[23] D. Huber, M. Reindl, S. F. Covre da Silva, C. Schimpf, J. Martín-Sánchez, H. Huang, G. Piredda, J. Edlinger, A. Rastelli, and R. Trotta, Strain-Tunable GaAs Quantum Dot: A Nearly Dephasing-Free Source of Entangled Photon Pairs on Demand, Phys. Rev. Lett. **121**, 033902 (2018).
[24] H. Wang, H. Hu, T.-H. Chung, J. Qin, X. Yang, J.-P. Li, R.-Z. Liu, H.-S. Zhong, Y.-M. He, X. Ding, Y.-H. Deng, Q. Dai, Y.-H. Huo, S. Höfling, C.-Y. Lu, and J.-W. Pan, On-Demand Semiconductor Source of Entangled Photons Which Simultaneously Has High Fidelity, Efficiency, and Indistinguishability, Phys. Rev. Lett. **122**, 113602 (2019).
[25] J. Liu, R. Su, Y. Wei, B. Yao, S. F. Covre da Silva, Y. Yu, J. Iles-Smith, K. Srinivasan, A. Rastelli, J. Li, and X. Wang, A solid-state source of strongly entangled photon pairs with high brightness and indistinguishability, Nat. Nanotechnol. **14**, 586 (2019).
[26] C. Hopfmann, W. Nie, N. L. Sharma, C. Weigelt, F. Ding, and O. G. Schmidt, Maximally entangled and gigahertz-clocked on-demand photon pair source, Phys. Rev. B **103**, 075413 (2021).
[27] A. Fognini, A. Ahmadi, M. Zeeshan, J. T. Fokkens, S. J. Gibson, N. Sherlekar, S. J. Daley, D. Dalacu, P. J. Poole, K. D. Jöns, V. Zwiller, and M. E. Reimer, Dephasing Free Photon Entanglement with a Quantum Dot, ACS Photonics **6**, 1656 (2019).
[28] S. Bounouar, C. de la Haye, M. Strauß, P. Schnauber, A. Thoma, M. Gschrey, J.-H. Schulze, A. Strittmatter, S. Rodt, and S. Reitzenstein, Generation of maximally entangled states and coherent control in quantum dot microlenses, Appl. Phys. Lett. **112**, 153107 (2018).
[29] D. Huber, M. Reindl, J. Aberl, A. Rastelli, and R. Trotta, Semiconductor quantum dots as an ideal source of polarization-entangled photon pairs on-demand: a review, J. Opt. **20**, 073002 (2018).
[30] A. Carmele and A. Knorr, Analytical solution of the quantum-state tomography of the biexciton cascade in semiconductor quantum dots: Pure dephasing does not affect entanglement, Phys. Rev. B **84**, 075328 (2011).
[31] M. Cygorek, F. Ungar, T. Seidelmann, A. M. Barth, A. Vagov, V. M. Axt, and T. Kuhn, Comparison of different concurrences characterizing photon pairs generated in the biexciton cascade in quantum dots coupled to microcavities, Phys. Rev. B **98**, 045303 (2018).
[32] T. Seidelmann, F. Ungar, M. Cygorek, A. Vagov, A. M. Barth, T. Kuhn, and V. M. Axt, From strong to weak temperature dependence of the two-photon entanglement resulting from the biexciton cascade inside a cavity, Phys. Rev. B **99**, 245301 (2019).
[33] S. Schumacher, J. Förstner, A. Zrenner, M. Florian, C. Gies, P. Gartner, and F. Jahnke, Cavity-assisted emission of polarization-entangled photons from biexcitons in quantum dots with fine-structure splitting, Opt. Express **20**, 5335 (2012).
[34] D. Heinze, A. Zrenner, and S. Schumacher, Polarization-entangled twin photons from two-photon quantum-dot emission, Phys. Rev. B **95**, 245306 (2017).
[35] T. Seidelmann, F. Ungar, A. M. Barth, A. Vagov, V. M. Axt, M. Cygorek, and T. Kuhn, Phonon-Induced Enhancement of Photon Entanglement in Quantum Dot-Cavity Systems, Phys. Rev. Lett. **123**, 137401 (2019).
[36] E. del Valle, Distilling one, two and entangled pairs of photons from a quantum dot with cavity QED effects and spectral filtering, New J. Phys. **15**, 025019 (2013).
[37] F. Troiani, J. I. Perea, and C. Tejedor, Cavity-assisted generation of entangled photon pairs by a quantum-dot cascade decay, Phys. Rev. B **74**, 235310 (2006).
[38] A. J. Hudson, R. M. Stevenson, A. J. Bennett, R. J. Young, C. A. Nicoll, P. Atkinson, K. Cooper, D. A. Ritchie, and A. J. Shields, Coherence of an Entangled Exciton-Photon State, Phys. Rev. Lett. **99**, 266802 (2007).
[39] C. Schimpf, M. Reindl, F. Basso Basset, K. D. Jöns, R. Trotta, and A. Rastelli, Quantum dots as potential sources of strongly entangled photons: Perspectives and challenges for applications in quantum networks, Appl. Phys. Lett. **118**, 100502 (2021).
[40] T. Seidelmann, C. Schimpf, T. K. Bracht, M. Cosacchi, A. Vagov, A. Rastelli, D. E. Reiter, and V. M. Axt, Two-Photon Excitation Sets Limit to Entangled Photon Pair Generation from Quantum Emitters, Phys. Rev. Lett. **129**, 193604 (2022).
[41] F. Basso Basset, M. B. Rota, M. Beccaceci, T. M. Krieger, Q. Buchinger, J. Neuwirth, H. Huet, S. Stroj, S. F. Covre da Silva, C. Schimpf, S. Höfling, T. Huber-Loyola, A. Rastelli, and R. Trotta, Signatures of the Optical Stark Effect on Entangled Photon Pairs from Resonantly-Pumped Quantum Dots, arXiv:2212.07087 [quant-ph] (2022).
[42] K. Edamatsu, Entangled photons: generation, observation, and characterization, Jpn. J. Appl. Phys. **46**, 7175 (2007).
[43] S. J. Freedman and J. F. Clauser, Experimental Test of Local Hidden-Variable Theories, Phys. Rev. Lett. **28**, 938 (1972).
[44] J. Park, T. Jeong, H. Kim, and H. S. Moon, Time-Energy Entangled Photon Pairs from Doppler-Broadened Atomic Ensemble via Collective Two-Photon Coherence, Phys. Rev. Lett. **121**, 263601 (2018).
[45] T. Seidelmann, M. Cosacchi, M. Cygorek, D. E. Reiter, A. Vagov, and V. M. Axt, Phonon-induced transition between entangled and nonentangled photon emission in constantly driven quantum-dot–cavity systems, Phys. Rev. B **107**, 075301 (2023).
[46] G. Lindblad, On the generators of quantum dynamical semigroups, Commun. Math. Phys. **48**, 119 (1976).
[47] L. Besombes, K. Kheng, L. Marsal, and H. Mariette, Acoustic phonon broadening mechanism in single quantum dot emission, Phys. Rev. B **63**, 155307 (2001).
[48] B. Krummheuer, V. M. Axt, and T. Kuhn, Theory of pure dephasing and the resulting absorption line shape in semiconductor quantum dots, Phys. Rev. B **65**, 195313 (2002).
[49] B. Krummheuer, V. M. Axt, T. Kuhn, I. D'Amico, and F. Rossi, Pure dephasing and phonon dynamics in GaAs- and GaN-based quantum dot structures: Interplay between material parameters and geometry, Phys. Rev. B **71**, 235329 (2005).
[50] D. E. Reiter, T. Kuhn, and V. M. Axt, Distinctive characteristics of carrier-phonon interactions in optically driven semiconductor quantum dots, Adv. Phys.: X **4**, 1655478

(2019).
[51] J. Förstner, C. Weber, J. Danckwerts, and A. Knorr, Phonon-Assisted Damping of Rabi Oscillations in Semiconductor Quantum Dots, Phys. Rev. Lett. **91**, 127401 (2003).
[52] P. Machnikowski and L. Jacak, Resonant nature of phonon-induced damping of Rabi oscillations in quantum dots, Phys. Rev. B **69**, 193302 (2004).
[53] A. Vagov, M. D. Croitoru, V. M. Axt, T. Kuhn, and F. M. Peeters, Nonmonotonic Field Dependence of Damping and Reappearance of Rabi Oscillations in Quantum Dots, Phys. Rev. Lett. **98**, 227403 (2007).
[54] D. P. S. McCutcheon, N. S. Dattani, E. M. Gauger, B. W. Lovett, and A. Nazir, A general approach to quantum dynamics using a variational master equation: Application to phonon-damped Rabi rotations in quantum dots, Phys. Rev. B **84**, 081305(R) (2011).
[55] N. Makri and D. E. Makarov, Tensor propagator for iterative quantum time evolution of reduced density matrices. I. Theory, J. Chem. Phys. **102**, 4600 (1995).
[56] N. Makri and D. E. Makarov, Tensor propagator for iterative quantum time evolution of reduced density matrices. II. Numerical methodology, J. Chem. Phys. **102**, 4611 (1995).
[57] A. Vagov, M. D. Croitoru, M. Glässl, V. M. Axt, and T. Kuhn, Real-time path integrals for quantum dots: Quantum dissipative dynamics with superohmic environment coupling, Phys. Rev. B **83**, 094303 (2011).
[58] A. M. Barth, A. Vagov, and V. M. Axt, Path-integral description of combined Hamiltonian and non-Hamiltonian dynamics in quantum dissipative systems, Phys. Rev. B **94**, 125439 (2016).
[59] M. Cygorek, A. M. Barth, F. Ungar, A. Vagov, and V. M. Axt, Nonlinear cavity feeding and unconventional photon statistics in solid-state cavity QED revealed by many-level real-time path-integral calculations, Phys. Rev. B **96**, 201201(R) (2017).
[60] D. F. V. James, P. G. Kwiat, W. J. Munro, and A. G. White, Measurement of qubits, Phys. Rev. A **64**, 052312 (2001).
[61] R. M. Stevenson, A. J. Hudson, A. J. Bennett, R. J. Young, C. A. Nicoll, D. A. Ritchie, and A. J. Shields, Evolution of Entanglement Between Distinguishable Light States, Phys. Rev. Lett. **101**, 170501 (2008).
[62] C. Sánchez Muñoz, F. P. Laussy, C. Tejedor, and E. del Valle, Enhanced two-photon emission from a dressed biexciton, New J. Phys. **17**, 123021 (2015).
[63] M. Cosacchi, M. Cygorek, F. Ungar, A. M. Barth, A. Vagov, and V. M. Axt, Path-integral approach for nonequilibrium multitime correlation functions of open quantum systems coupled to Markovian and non-Markovian environments, Phys. Rev. B **98**, 125302 (2018).
[64] H. Carmichael, ed., *An Open Systems Approach to Quantum Optics* (Springer, Berlin, 1993).
[65] M. Cosacchi, T. Seidelmann, M. Cygorek, A. Vagov, D. E. Reiter, and V. M. Axt, Accuracy of the Quantum Regression Theorem for Photon Emission from a Quantum Dot, Phys. Rev. Lett. **127**, 100402 (2021).
[66] D. P. S. McCutcheon, Optical signatures of non-Markovian behavior in open quantum systems, Phys. Rev. A **93**, 022119 (2016).
[67] K. Roy-Choudhury and S. Hughes, Quantum theory of the emission spectrum from quantum dots coupled to structured photonic reservoirs and acoustic phonons, Phys. Rev. B **92**, 205406 (2015).
[68] J. Iles-Smith, D. P. S. McCutcheon, A. Nazir, and J. Mørk, Phonon scattering inhibits simultaneous near-unity efficiency and indistinguishability in semiconductor single-photon sources, Nat. Photonics **11**, 521 (2017).
[69] A. Reigue, J. Iles-Smith, F. Lux, L. Monniello, M. Bernard, F. Margaillan, A. Lemaitre, A. Martinez, D. P. S. McCutcheon, J. Mørk, R. Hostein, and V. Voliotis, Probing Electron-Phonon Interaction through Two-Photon Interference in Resonantly Driven Semiconductor Quantum Dots, Phys. Rev. Lett. **118**, 233602 (2017).
[70] M. Cosacchi, T. Seidelmann, M. Cygorek, A. Vagov, D. E. Reiter, and V. M. Axt, Erratum: Accuracy of the Quantum Regression Theorem for Photon Emission from a Quantum Dot [Phys. Rev. Lett. 127, 100402 (2021)], Phys. Rev. Lett. **128**, 079901(E) (2022).
[71] W. K. Wootters, Entanglement of Formation of an Arbitrary State of Two Qubits, Phys. Rev. Lett. **80**, 2245 (1998).
[72] W. K. Wootters, Entanglement of formation and concurrence, Quantum Inf. Comput. **1**, 27 (2001).
[73] D. Stefanatos and E. Paspalakis, Rapid biexciton-state preparation in a quantum dot using on-off pulse sequences, Phys. Rev. A **102**, 052618 (2020).
[74] B. U. Lehner, T. Seidelmann, G. Undeutsch, C. Schimpf, S. Manna, M. Gawełczyk, S. F. Covre da Silva, X. Yuan, S. Stroj, D. E. Reiter, V. M. Axt, and A. Rastelli, Beyond the Four-Level Model: Dark and Hot States in Quantum Dots Degrade Photonic Entanglement, Nano Lett. **23**, 1409 (2023).
[75] M. Glässl, M. D. Croitoru, A. Vagov, V. M. Axt, and T. Kuhn, Influence of the pulse shape and the dot size on the decay and reappearance of Rabi rotations in laser driven quantum dots, Phys. Rev. B **84**, 125304 (2011).
[76] S. Lüker, T. Kuhn, and D. E. Reiter, Phonon impact on optical control schemes of quantum dots: Role of quantum dot geometry and symmetry, Phys. Rev. B **96**, 245306 (2017).